Hindawi
Journal of Chemistry
Volume 2021, Article ID 9378490, 11 pages
https://doi.org/10.1155/2021/9378490

Research Article

Characterization of Commercial TiO_2 P90 Modified with ZnO by the Impregnation Method

Tetiana A. Dontsova,[1] **Olena I. Yanushevska**,[1] **Svitlana V. Nahirniak**,[1] **Anastasiya S. Kutuzova**,[1] **Grigory V. Krymets**,[1] **and Petro S. Smertenko**[2]

[1]*Department of Technology of Inorganic Substances, Water Purification and General Chemical Technology, National Technical University of Ukraine "Igor Sikorsky Kyiv Polytechnic Institute", Kyiv 03056, Ukraine*
[2]*Department of Optoelectronics, Institute of Semiconductor Physics NAS of Ukraine, Kyiv 03680, Ukraine*

Correspondence should be addressed to Tetiana A. Dontsova; dontsova@xtf.kpi.ua

Received 26 July 2020; Revised 9 February 2021; Accepted 29 March 2021; Published 7 April 2021

Academic Editor: Shafaqat Ali

This article is devoted to TiO_2/ZnO nanocomposites' creation by modifying with the commercial TiO_2/P90 product using the impregnation method and identifying the effect of the ZnO modifier on its adsorption, structural, photocatalytic, and electrical properties. The synthesized TiO_2/ZnO nanocomposites were characterized by XRD, XRF, XPS, and low-temperature nitrogen adsorption-desorption methods. As a result, nanostructured TiO_2/ZnO composites with the ZnO content of 2, 5, 10, and 15% were obtained. It was shown that the phase composition of TiO_2/P90 does not change during the nanocomposite synthesis. XPS studies of TiO_2/ZnO nanocomposites indicated the presence of Ti^{4+}, Zn^{2+}, O^{2-}, and OH states on their surface, which is associated with TiO_2, ZnO, and hydroxide ions. The nitrogen adsorption-desorption method showed that the commercial TiO_2/P90 sample is nonporous, and all TiO_2/ZnO nanocomposites are characterized by almost the same homogeneous mesoporous structure. Experimentally established sorption and photocatalytic properties depend on the specific surface area and electrostatic interaction with dyes. The effect of the ZnO modifier on I-V characteristics of the TiO_2/P90 sample was revealed. The obtained experimental data showed that the TiO_2/P90 sample contains one type of current carriers, and TiO_2/2ZnO and TiO_2/5ZnO nanocomposites are characterized by two types of current carriers.

1. Introduction

Semiconductor nanomaterials based on metal oxides have recently attracted more and more attention due to their interesting properties. They can be successfully used in applied ecology, in particular, as catalysts, photocatalysts, and other materials where their unique electrical properties are required [1–4].

One of the well-known semiconductor metal oxide nanomaterials is titanium (IV) oxide (TiO_2), as evidenced by more than 20,000 publications on TiO_2 in ScienceDirect over the past 5 years. TiO_2 forms several structural modifications, the main of which are tetragonal (rutile and anatase) and orthorhombic (brookite). Among them, anatase and rutile modifications are the most widely recognized in the scientific community as a promising nanomaterial for environmental applications [5].

Heterogeneous photocatalysis is the most popular application of TiO_2. It is well known that the ultimate photoefficiency of each photocatalyst strongly depends on its physicochemical properties such as specific surface area, particle size, and phase composition, as well as on the synthesis method and precursors' type used to obtain it [6–11]. Another potential TiO_2 application is sensory, where it can be successfully used as a sensitive chemoresistive layer of gas sensors [12–14]. The use of TiO_2 in photovoltaics is also promising and practically significant [15, 16]. These are only a few examples of titanium (IV) oxide applications, based on prominent characteristics of TiO_2 such as structural, adsorption, (photo) catalytic, and electrical properties,

which, depending on the synthesis conditions, can differ significantly [17–19].

Adjustment of physicochemical properties of titanium (IV) oxide is also possible by doping, modifying, and creating TiO_2-based nanocomposites [20–28]. In all cases, it is quite feasible to implement desired improvements in order to obtain certain physical and chemical properties. Creation of nanocomposites based on TiO_2 is extremely promising due to the extension of the "life" of photoexcited "electron-hole" pairs in comparison with pure metal oxides [29–32]. To obtain TiO_2-based nanocomposites, the following semiconductor materials are usually used: ZnO, Fe_2O_3, WO_3, CdS, ZnS, Cu_2O, CuO SnO_2, and V_2O_5, among which zinc oxide stands out [28].

ZnO crystallizes in three crystalline structures—cubic rock salt, cubic zinc blende, and hexagonal wurtzite—among which only the latter is thermodynamically stable under normal conditions. ZnO is characterized by unique electrical and optical properties that allow its successful environmental application, namely, as a photocatalyst, which has long competed with the most popular TiO_2, and as a sensitive layer of gas sensors [33, 34].

It is known that both titanium (IV) oxide and zinc oxide are n-type broadband semiconductors with a bandgap of 3.2 eV (anatase) and 3.37 eV, respectively. They have similar physicochemical properties and characteristics such as nontoxicity, high photoactivity, and low cost [35–37]. However, high photoactivity of both TiO_2 and ZnO is limited by absorption of wavelengths not exceeding 385 nm and high recombination rate of "electron-hole" pairs [37]. It is reported that a significant improvement in optical and photochemical properties can be achieved by creating nanostructures with both TiO_2 and ZnO due to better charge separation in them [35–38]. Besides, it is noted that the obtainment of nanocomposites of different TiO_2/ZnO morphology results in nanocomposite structures capable to absorb wavelengths in the visible light region [38]. Thus, the similarity of TiO_2 and ZnO properties can make their combined use in the form of nanocomposites a successful solution to the problems of low concentration of charged carriers, high recombination rate of "electron-hole" pairs, light absorption difficulty in the visible region, etc.

Various researchers have shown that, in order to create effective nanocomposite photocatalysts, it is necessary to vary synthesis methods, particle morphology, surface chemistry, degree of crystallinity/amorphousness, mass ratios of components in the TiO_2-ZnO system, etc. [39–41]. Increased photostability, accompanied by improved catalytic activity, is one of the factors justifying the creation of nanocomposites of mixed (binary) oxides, which are considered as promising photocatalysts for environmental applications. Such materials can also be used in lithium batteries, supercapacitors, and fuel cells [42]. The interaction of TiO_2 and ZnO in nanocomposite structures is expected to improve physical and chemical properties (such as electrical conductivity and charge carrier concentration) compared to individual phases of pure oxides [43]. Thus, creation of binary structures, namely, TiO_2-ZnO, will promote the formation of new nanocomposite materials with new and/or improved characteristics. Although several studies on the creation and investigation of TiO_2-ZnO nanocomposites have been presented in the literature to date, it is still unclear how ZnO and its content affect photocatalytic and electrical properties. Therefore, additional research on the effect of ZnO on the TiO_2 characteristics will provide a better understanding of the change in its properties to purposefully alter them.

To obtain such binary nanocomposites and study their photocatalytic and electrical properties, the use of commercial TiO_2 samples is of particular interest, which are widely available and already well studied in the literature [44, 45]. Among commercial photocatalysts, TiO_2 P25 (Evonik, Germany) is widely used as a reference of its thorough studies [46–48]. However, in our opinion, the commercial product of TiO_2 P90 from the same company may be a more interesting material for creating adsorbents, (photo) catalysts, gas sensor sensitive layers, and other functional materials due to the larger specific surface area [44]. P90 is characterized by almost 2 times higher specific surface area (90–110 m^2/g) compared to P25 (50–70 m^2/g). The average size of P90 particles is smaller (~30 nm) than in the P25 sample (~50 nm), and the content of the anatase phase in the P90 sample is slightly higher (91–92%) than that in P25 TiO_2 (87–88%).

Therefore, the current work is aimed at the modification of the commercial product TiO_2 P90 with zinc oxide by a simple impregnation method to obtain TiO_2-ZnO nanocomposites and to evaluate the effect of the ZnO modifier on the adsorption, structural, photocatalytic, and electrical properties of TiO_2 P90.

2. Materials and Methods

2.1. Materials. The following reagents were used in the work: titanium (IV) oxide (TiO_2, Aeroxide® TiO_2 P90, Evonik, Germany); zinc nitrate ($Zn(NO_3)_2$•$6H_2O$, Merck KGaA, Germany); nitric acid (HNO_3, 65%, Merck KGaA, Germany); methylene blue dye ($C_{16}H_{18}ClN_3S$, Carlo Erba Reagents, France); and Congo red dye ($C_{32}H_{22}N_6Na_2O_6S_2$, Carlo Erba Reagents, France). All used reagents were of high chemical purity grade.

2.2. Synthesis. The synthesis of nanocomposites was performed by the impregnation method [49]. 10 mL of zinc nitrate solution was added dropwise under stirring to 1 g of TiO_2. Concentration of zinc nitrate solution was calculated so that it corresponded to 2, 5, 10, and 15% of ZnO in the final nanocomposite. The resulting suspensions were first left for 12 hours, then dried at 100°C for 60 minutes, and calcined at 500°C for 60 minutes. As a result, samples labeled TiO_2/2ZnO, TiO_2/5ZnO, TiO_2/10ZnO, and TiO_2/15ZnO were obtained, respectively.

2.3. Characterization of P*90 and TiO_2/ZnO Nanocomposites.* The phase composition determination of the studied samples was performed on an X-ray diffractometer (Rigaku Ultima IV (Japan)) with CuKα radiation (40 kW, 30 mA). Calculations were done automatically using standard cards: № 01-078-4187 (rutile), № 01-070-7348 (anatase), and № 01-077-

0191 (wurtzite). The chemical composition of the synthesized nanocomposites was determined by the X-ray fluorescence method using the analyzer EXPERT 3L IHAM (Ukraine). X-ray photoelectron spectroscopy spectra were obtained using Kratos AXIS-165 spectrometer (England) with Al mono Kalfa X-ray. Nitrogen adsorption-desorption isotherms were obtained on Quantachrome® Nova 4200e (USA). Sorption and photocatalytic properties were evaluated by the discoloration degree of dyes of different nature (methylene blue (MB), $C_{16}H_{18}ClN_3S$, or Congo red (CR), $C_{32}H_{22}N_6Na_2O_6S_2$).

Volt-ampere characteristics (I-V characteristics) of the studied samples were measured in the quasi-stationary mode using an automated tester 14TKC-100 both in the dark and under illumination 0.03 AM0. For this, the powders were placed between two clear glass plates with ITO electrodes and a resistance of 30 Ohm/□, and the distance between the plates was 2 μm.

3. Results and Discussion

3.1. XRD and Chemical Composition. Figure 1 presents diffraction patterns of samples TiO_2/P90, TiO_2/2ZnO, TiO_2/5ZnO, TiO_2/10ZnO, and TiO_2/15ZnO, respectively.

According to the presented diffractograms, the phases of anatase and rutile are observed for the TiO_2/P90 sample; for TiO_2/ZnO nanocomposites in all cases, there are phases of anatase, rutile, and wurtzite (ZnO).

Table 1 shows the phase composition (automatically calculated by the PDXL software package), ZnO content (determined by the X-ray fluorescence method), and the crystallite size (calculated by the Scherrer equation). The presented phase composition for the TiO_2/P90 sample and TiO_2/ZnO nanocomposites indicates that the modification and synthesis temperature (500°C) do not change the phase composition of TiO_2/P90.

X-ray phase and X-ray fluorescence analysis methods (Table 1) confirm the theoretically calculated content of zinc oxide in nanocomposites. The ZnO content is 2, 5, 10, and 15%. The average crystallite size for all samples is in the range of 5.1–6.9 nm for TiO_2 and 3.4–6.0 nm for ZnO. Thus, it can be stated that TiO_2/ZnO nanocomposites with the theoretically calculated ZnO content were obtained without changing the phase composition of TiO_2/P90.

3.2. XPS. Surface states of TiO_2/ZnO nanocomposites were evaluated by X-ray photoelectron spectroscopy, resulting in XPS spectra, which are shown in Figure 2. The survey spectra of TiO_2/ZnO nanocomposites (Figure 2(a)) indicate the presence of Ti, Zn, O, and C (hydrocarbons from the XPS device). Native XPS spectra of Ti 2p, Zn 2p, and O 1s for TiO_2/ZnO nanocomposites are shown in Figures 2(b), 2(c), and 2(d), respectively. The XPS data report showed the presence of Ti^{4+} for titanium, Zn^{2+} for zinc, and O^{2-} for oxygen on the surface of nanocomposites.

The spectrum for Ti 2p (Figure 2(b)) contains two peaks: the first one at about 458.5 eV refers to the binding energy of Ti 2p3/2, and the second one at about 464 eV corresponds to the binding energy of Ti 2p1/2 [30]. For all nanocomposites, the XPS Zn 2p spectra (Figure 2(c)) also show two peaks approximately at 1021.1 eV and 1044 eV, which are characteristics of Zn 2p3/2 and Zn 2p1/2, respectively [50–52]. The absence of other Zn 2p peaks indicates that zinc ions form ZnO and that they are not part of the TiO_2 lattice. The XPS O 1s spectra (Figure 2(d)) for all nanocomposites are also identical and are characterized by peaks at 529.2 eV and 531.7 eV, which correspond to oxygen bound in the crystal lattice of metal oxides and hydroxyl oxygen (OH) on the sample surface, respectively [53].

Thus, the study of TiO_2/ZnO nanocomposites by XPS analysis revealed the surface element compositions: Ti^{4+} for titanium, Zn^{2+} for zinc, and O^{2-} for oxygen. In addition, the presence of hydroxide ions (OH) on their surface was found.

3.3. Structural and Adsorption Characteristics. Figure 3 displays nitrogen adsorption-desorption isotherms for all samples. As can be seen from the isotherms, the TiO_2/P90 sample and TiO_2/ZnO nanocomposites have different porous structures.

Thus, according to the IUPAC classification [54], the TiO_2/P90 sample has type III adsorption isotherm, which is a characteristic of nonporous or macroporous materials. The isotherms of all samples modified with zinc oxide have a slightly different form; the isotherm of type III is transformed into type V, namely, to V (a). This indicates a transition from a nonporous structure to a mesoporous one, which developed as a result of the modification.

Analyzing the resulting hysteresis loops in TiO_2/ZnO nanocomposites, it can be noted that they belong to type H2 (b), although being very similar to type H1 [54]. The reason for this might be that nanocomposites have open ink-bottle pores that are homogeneous and have approximately the same neck size and pore width.

The pore size distribution for all samples is shown in Figure 4, which confirms the presence of a nonporous structure for TiO_2/P90 and the appearance of mesopores of almost the same size for TiO_2/ZnO nanocomposites.

Specific surface areas determined by the Brunauer–Emmett–Teller (BET) equation decrease from 113 m^2/g to 60 m^2/g with the increase in the ZnO content (Table 2). This indicates the aggregation of titanium (IV) oxide particles during modification and heat treatment. Obtained by the Barrett–Joyner–Halenda (BJH) method, the average pore diameter for all samples correlates with the obtained isotherm types and porous structures and is in the range of 6.8–10.8 nm.

3.4. Adsorption and Photocatalytic Properties. Adsorption-photocatalytic properties were investigated by the discoloration degree of aqueous dye solutions (methylene blue at 664 nm and Congo red at 505 nm), which was determined by the following equation (%) [31]:

$$X = \frac{A_0 - A_1}{A_0} \times 100, \quad (1)$$

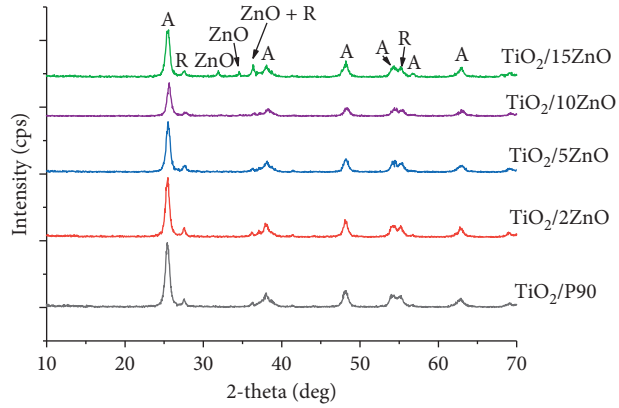

Figure 1: Diffraction patterns of TiO_2/P90 and TiO_2/ZnO nanocomposites.

Table 1: Diffraction analysis data and ZnO content in nanocomposites.

Sample	TiO_2/P90	TiO_2/2ZnO	TiO_2/5ZnO	TiO_2/10ZnO	TiO_2/15ZnO
Phase composition (%)	91 (A) 9 (R)	88.5 (A) 10 (R) 1.5 (ZnO)	86 (A) 9.5 (R) 4.5 (ZnO)	83 (A) 7.5 (R) 9.5 (ZnO)	77 (A) 7 (R) 16 (ZnO)
ZnO content* (%)	0	1.97	5.01	9.95	15.02
Average crystallite size (nm)	5.1 (TiO_2)	5.3 (TiO_2)	5.2 (TiO_2)	5.9 (TiO_2) 3.4 (ZnO)	6.9 (TiO_2) 6.0 (ZnO)

*Calculated from X-ray fluorescence analysis.

where A_0 is the optical density of the initial dye solution and A_1 is the optical density of the solution after adsorption/photocatalysis.

The results of adsorption-photocatalytic studies are presented in Table 3.

It can be seen that both TiO_2/P90 sample and TiO_2/ZnO nanocomposites have low sorption activity towards the cationic dye MB (0–7%) and high sorption activity towards the anionic dye CR (82–96%). It is probably associated with the negative charge of their surface [30] and the corresponding electrostatic interaction between the surface of nanocomposites and dyes. In this case, as a result of the sorption interaction of the studied samples with MB, there is low dye removal efficiency on the TiO_2/5ZnO sample, and there is low removal efficiency of CR on TiO_2/2ZnO.

Photocatalytic removal of MB from the aqueous solution is significantly different from the sorption experiments. It is characterized by a greater discoloration degree, which is 19–91%, and decreases with the increase in the zinc oxide content. This fact correlates well with the change in the specific surface area. Photocatalytic discoloration of CR is in accordance with the sorption removal of this dye on TiO_2/P90 and TiO_2/ZnO nanocomposites and is slightly higher, which indicates, first of all, strong electrostatic interaction of the studied samples with the anionic dye.

3.5. Electrical Characteristics. I-V characteristics measured for three samples of TiO_2/P90, TiO_2/2ZnO, and TiO_2/5ZnO are shown in Figures 5–7, respectively. These two nanocomposites were chosen for the study because of the similarity of their properties with TiO_2/10ZnO and TiO_2/15ZnO samples in terms of adsorption and structural characteristics and their better sorption-photocatalytic properties.

Additionally, dimensionless sensitivity (α) was calculated for the studied samples by determining the slope of the curves in the double logarithmic scale (log-log scale) according to the equation $\alpha = dl\ gI/d\lg V$. Thus, analyzing the I-V characteristics, we can see that all samples have both common features and differences. General features include the following phenomena. At high applied voltages, both in the dark and under the illumination, I-V characteristics almost merge, which indicates that injection processes mainly take place at the grain boundaries. Conductivity at high voltage is almost linear, which is also further confirmed by the value of dimensionless sensitivity $\alpha = 1$. Besides, photosensitivity in the low-voltage range was detected for all samples. In general, I-V curves of all samples in the region up to 1 V are predominantly nonlinear, where the superlinear sections alternate with the sublinear sections several times.

The differences found in the samples are interesting. Thus, individual features of pure titanium (IV) oxide TiO_2/P90 show the presence of the region with $\alpha = 0.75$ slope in the dark in the low-voltage region. When illuminated, I-V characteristics become sublinear with $\alpha = 0.5$, which is a characteristic of rectifying I-V characteristic. For the I-V curve obtained in the dark, there are regions with $\alpha = 2.0$ that is a characteristic of monomolecular recombination when one type of current carriers dominates. When illuminated, a region with $\alpha = 1.5$ appears on the I-V curve, which is a

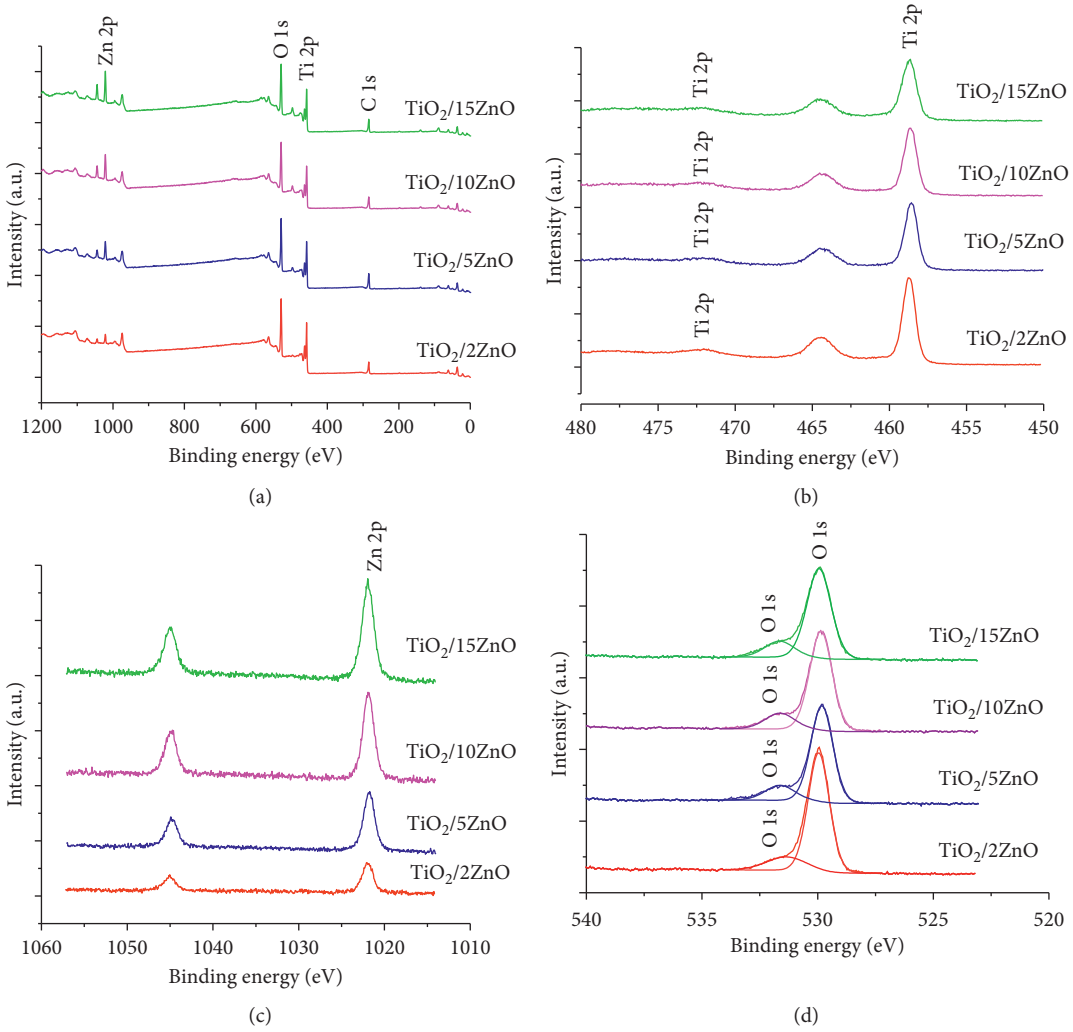

Figure 2: XPS spectra of TiO_2-ZnO nanocomposites: (a) survey, (b) Ti 2p, (c) Zn 2p, and (d) O 1s.

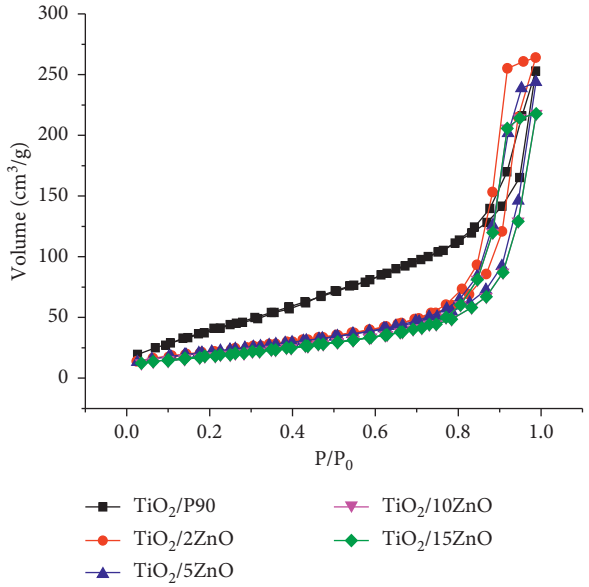

Figure 3: Nitrogen adsorption-desorption isotherms of TiO_2/P90 and TiO_2/ZnO nanocomposites.

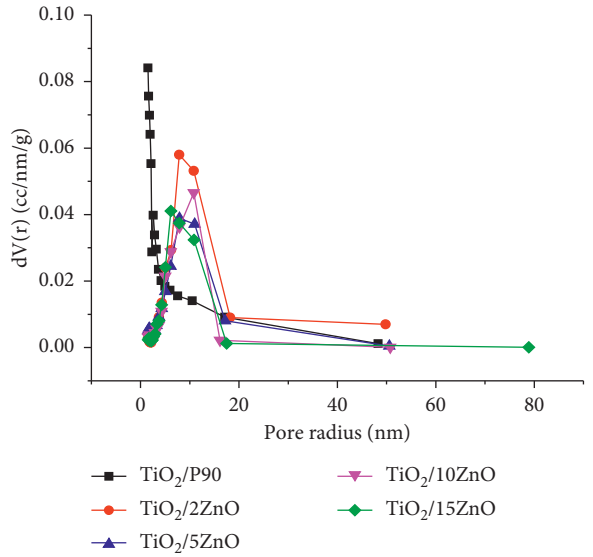

Figure 4: Pore size distribution of TiO_2/P90 and TiO_2/ZnO nanocomposites.

Table 2: Structural and adsorption characteristics of TiO_2/ZnO nanocomposites.

Sample	TiO_2/P90	TiO_2/2ZnO	TiO_2/5ZnO	TiO_2/10ZnO	TiO_2/15ZnO
S (m^2/g)	113	78	75	65	60
Average pore diameter (nm)	—	7.9	7.9	10.8	6.8

Table 3: Adsorption-photocatalytic characteristics of TiO_2/ZnO nanocomposites.

Sample	TiO_2/P90	TiO_2/2ZnO	TiO_2/5ZnO	TiO_2/10ZnO	TiO_2/15ZnO
Discoloration degree (X): sorption/photocatalysis (%)					
Methylene blue	0/91	4/77	7/51	0/44	0/19
Congo red	95/98	96/100	91/95	88/91	82/87

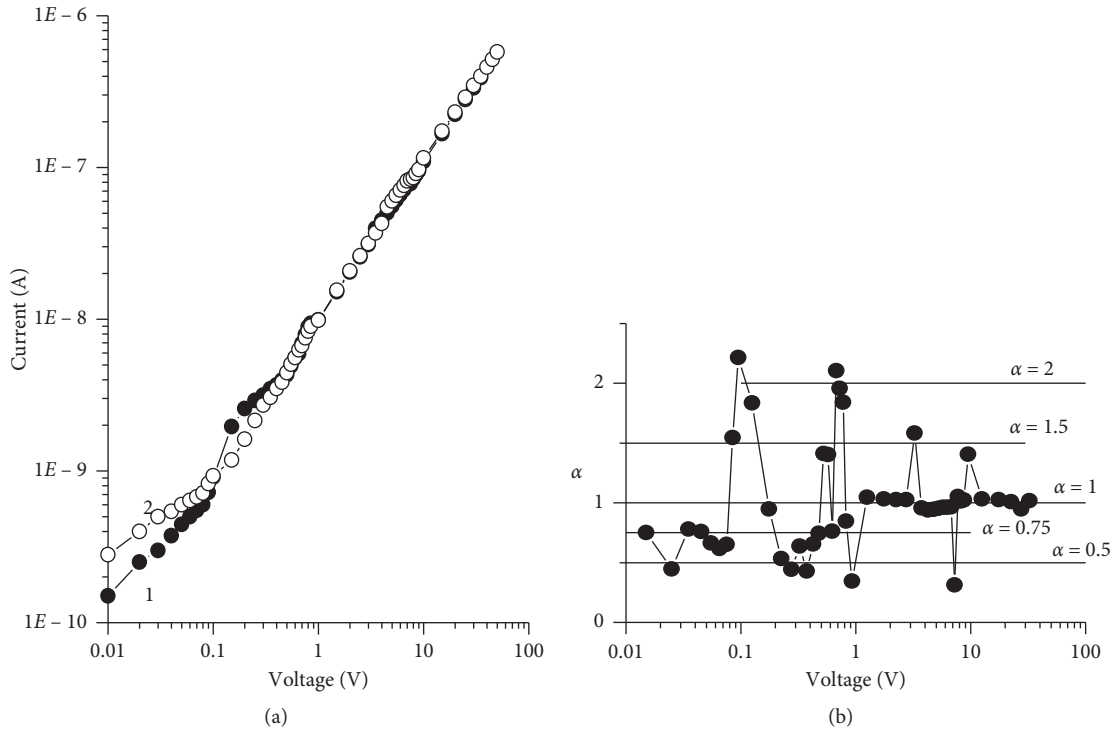

Figure 5: Continued.

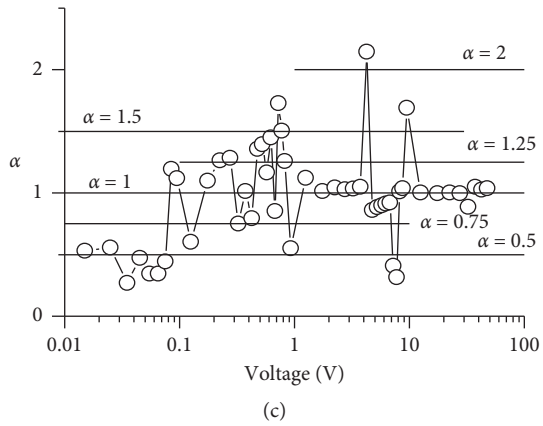

(c)

Figure 5: I-V characteristics (a) and their dimensionless sensitivity (b, c) of the TiO_2/P90 sample: 1-in the dark (b) and 2-under illumination (c).

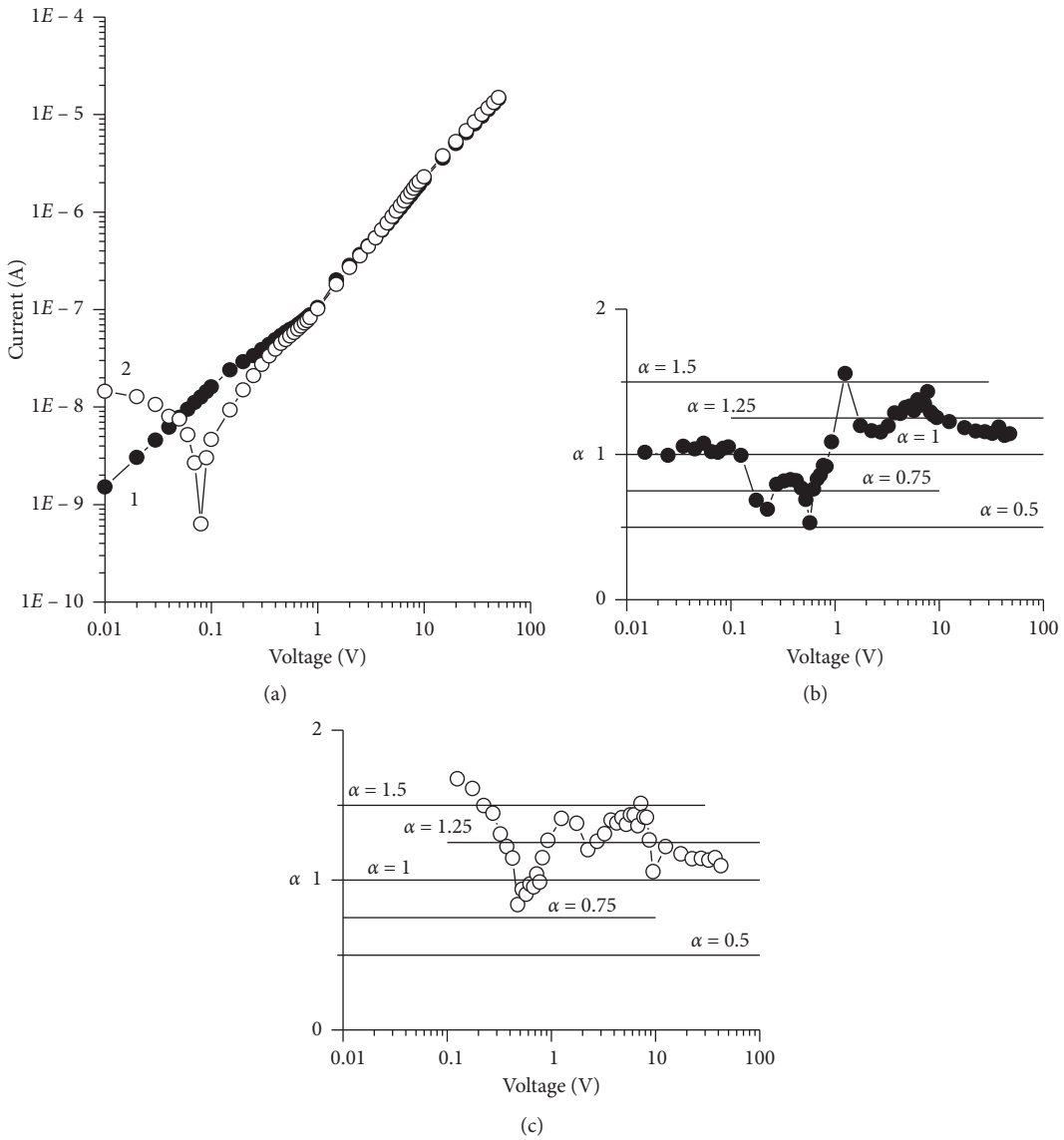

Figure 6: I-V characteristics (a) and their dimensionless sensitivity (b, c) of the TiO_2/2ZnO sample: 1-in the dark (b) and 2-under illumination (c).

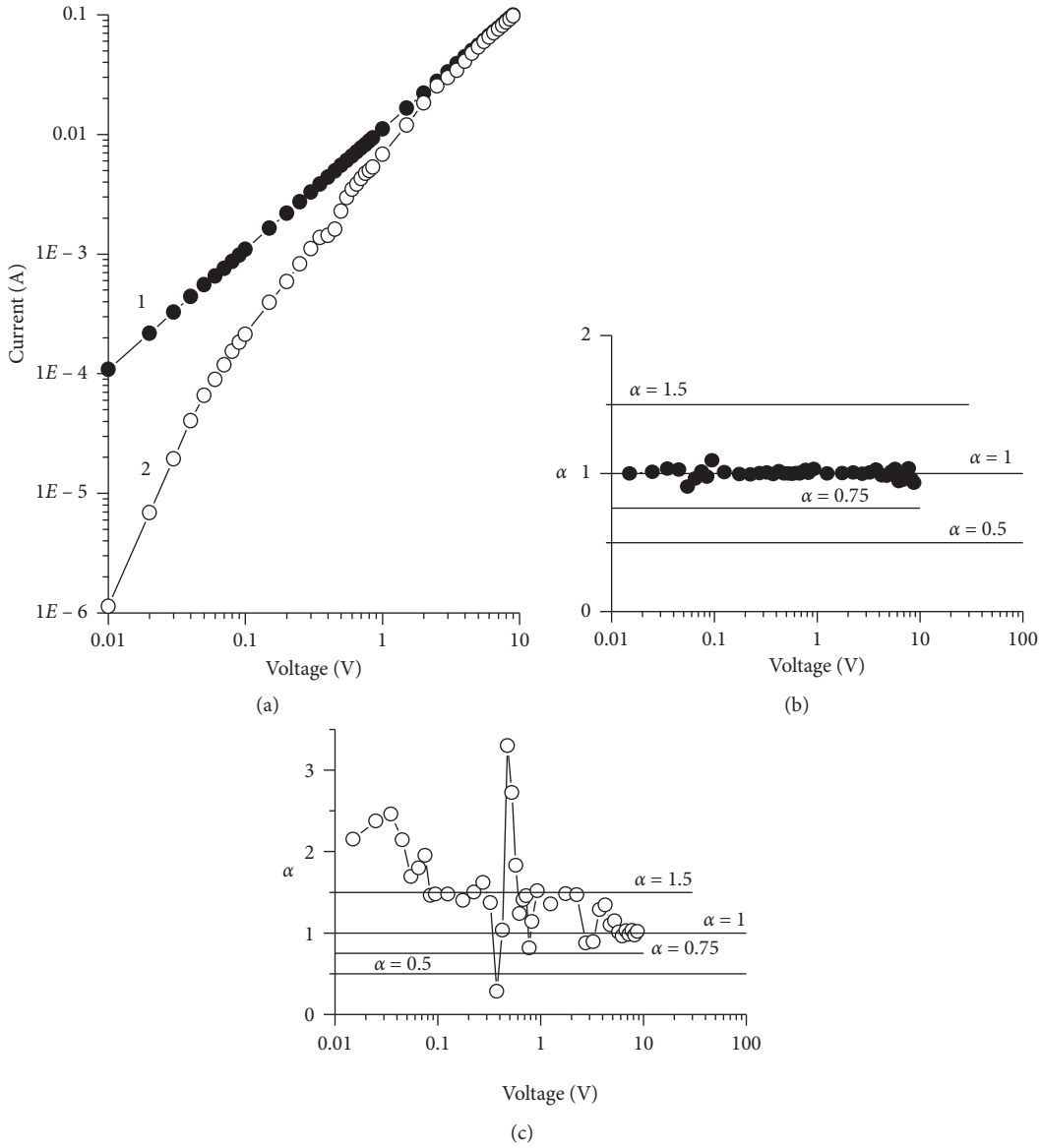

Figure 7: I-V characteristics (a) and their dimensionless sensitivity (b, c) of the TiO2/5ZnO sample: 1-in the dark (b) and 2-under illumination (c).

characteristic of bimolecular recombination, when the concentrations of the main and nonbasic current carriers are close to each other. That is, illumination facilitates the injection of nonbasic current carriers from the anode contact. The ratio of currents in the light and in the dark is 6.

The TiO_2/2ZnO sample has slightly different features. Thus, the addition of ZnO in the amount of 2% increases the current almost by one order of magnitude in the dark, and I-V characteristics are also characterized by a region with $\alpha = 0.75$. I-V characteristics of the TiO_2/2ZnO sample under the illumination have a photovoltaic region, and both I-V characteristics have areas with $\alpha = 1.5$, which is typical of bimolecular recombination, so the addition of ZnO promotes the injection of nonbasic current carriers.

Further increase of the ZnO content to 5% in pure titanium (IV) oxide significantly increases, up to five orders, the current in the dark compared to TiO_2/2ZnO. I-V characteristics for this sample are linear with $\alpha = 1$ in the entire applied voltage range. I-V characteristics of the TiO_2/5ZnO sample under illumination are also characterized by $\alpha = 1.5$, which is inherent in bimolecular recombination.

Thus, it can be stated that the addition of ZnO to TiO_2 changes both quantitative and qualitative parameters of I-V characteristics of the TiO_2/P90 sample. The photovoltaic effect in the presence of 2% ZnO and the inversion of the light current in case of 5% ZnO concentration are unusual. The found regularities indicate the prospects of using the TiO_2/P90 sample in structures for which there must be one type of current carriers, for example, photoresistors and sensors based on the effect of the main current carrier injection. TiO_2/2ZnO and TiO_2/5ZnO can be used in

structures for which two types of current carriers are required, for example, in the converters of solar energy into electricity.

4. Conclusions

TiO_2/ZnO nanocomposites were obtained by impregnating commercial TiO_2/P90 manufactured by Evonik in order to determine the effect of the ZnO modifier on the adsorption, structural, photocatalytic, and electrical properties of the nanocomposites. The obtained nanocomposites were characterized by XRD, XRF, XPS, and low-temperature nitrogen adsorption-desorption method, and their sorption, photocatalytic, and electrical properties were investigated.

It was found that modification does not change the phase composition of TiO_2/P90, and the ZnO content determined by diffraction and X-ray fluorescence methods corresponds to the theoretically calculated one. In all cases, nanostructured TiO_2/ZnO composites were obtained (crystallite sizes in the range of 3.4–6.9 nm).

The study of the surface chemical states of TiO_2/ZnO nanocomposites by XPS analysis revealed the degree of oxidation on their surface: Ti^{4+} for titanium, Zn^{2+} for zinc, and O^{2-} for oxygen. Besides, the presence of hydroxide ions (OH) on their surface was found.

Studies of the adsorption and structural characteristics of TiO_2/ZnO nanocomposites have shown that the commercial TiO_2/P90 sample is nonporous. Its modification with zinc oxide leads to the aggregation of TiO_2 particles and the development of mesoporosity. As a result, the specific surface area of TiO_2/P90 decreases (from 113 m^2/g to 60 m^2/g) with the following dependence: the higher the ZnO content, the smaller the specific surface area.

The results of sorption-photocatalytic experiments point at better adsorption properties towards the anionic dye and better photocatalytic activity towards the cationic dye that decreases with the increase in the ZnO content, which correlates well with the data on the specific surface area. The study of electrical properties indicates a significant effect of ZnO on the quantitative and qualitative I-V characteristics of the TiO_2/P90 sample. The established regularities allow stating the prospects of using the TiO_2/P90 sample in structures, for which one type of current carriers is required (for example, photoresistors and sensors). TiO_2/2ZnO and TiO_2/5ZnO nanocomposites can be effectively used in structures, for which two types of current carriers are required (for example, for converters of solar energy into electricity).

Data Availability

All the data generated and/or analyzed during this study are included within this published article.

Conflicts of Interest

The authors declare that there are no conflicts of interest regarding the publication of this paper.

References

[1] S. Banerjee, A. Zangiabadi, A. Mahdavi-Shakib et al., "Quantitative structural characterization of catalytically active TiO_2 nanoparticles," *ACS Applied Nano Materials*, vol. 2, no. 10, pp. 6268–6276, 2019.

[2] J.-Y. Bottero, M. Auffan, J. Rose et al., "Manufactured metal and metal-oxide nanoparticles: properties and perturbing mechanisms of their biological activity in ecosystems," *Comptes Rendus Geoscience*, vol. 343, no. 2-3, pp. 168–176, 2011.

[3] T. A. Dontsova, S. V. Nahirniak, and I. M. Astrelin, "Metaloxide nanomaterials and nanocomposites of ecological purpose," *Journal of Nanomaterials*, vol. 2019, Article ID 5942194, 31 pages, 2019.

[4] H. L. Tuller, "Review of electrical properties of metal oxides as applied to temperature and chemical sensing," *Sensors and Actuators*, vol. 4, pp. 679–688, 1983.

[5] J. Moma and J. Baloyi, "Modified titanium dioxide for photocatalytic applications," in *Photocatalysts-Applications and Attributes*, S. Bahadar Khan and K. Akhtar, Eds., IntechOpen, London, UK, 2019.

[6] A. Fujishima, T. N. Rao, and D. A. Tryk, "Titanium dioxide photocatalysis," *Journal of Photochemistry and Photobiology C: Photochemistry Reviews*, vol. 1, no. 1, pp. 1–21, 2000.

[7] A. Kutuzova and T. Dontsova, "Synthesis, characterization and properties of titanium dioxide obtained by hydrolytic method," in *Proceedings of the 2017 IEEE 7th International Conference on Nanomaterials: Applications and Properties*, pp. 286–290, Zatoka, Ukraine, September 2017.

[8] M. H. Habibi, M. N. Esfahani, and T. A. Egerton, "Photochemical characterization and photocatalytic properties of a nanostructure composite TiO_2 film," *International Journal of Photoenergy*, vol. 2007, Article ID 13653, 8 pages, 2007.

[9] T. Dontsova, I. Ivanenko, and I. Astrelin, "Synthesis and characterization of titanium (IV) oxide from various precursors," *Springer Proceedings in Physics*, vol. 167, pp. 275–293, 2015.

[10] K. Qi, B. Cheng, J. Yu, and W. Ho, "A review on TiO_2-based Z-scheme photocatalysts," *Chinese Journal of Catalysis*, vol. 38, no. 12, pp. 1936–1955, 2017.

[11] A. Sviderskyi, S. Nahirniak, T. Yashchenko et al., "Properties of TiO_2 and SnO_2 in a state of different dispersion and morphology," in *Proceedings of the 2018 IEEE 8th International Conference Nanomaterials: Application and Properties*, pp. 1–4, Zatoka, Ukraine, September 2018.

[12] Z. Li, Z. Yao, A. A. Haidry et al., "Resistive-type hydrogen gas sensor based on TiO_2: a review," *International Journal of Hydrogen Energy*, vol. 43, no. 45, pp. 21114–21132, 2018.

[13] J. Yu, J. Lei, L. Wang, J. Zhang, and Y. Liu, "TiO_2 inverse opal photonic crystals: synthesis, modification, and applications-a review," *Journal of Alloys and Compounds*, vol. 769, pp. 740–757, 2018.

[14] X. Gao and T. Zhang, "An overview: facet-dependent metal oxide semiconductor gas sensors," *Sensors and Actuators B: Chemical*, vol. 277, pp. 604–633, 2018.

[15] D. Sinha, D. De, D. Goswami, A. Mondal, and A. Ayaz, "ZnO and TiO_2 nanostructured dye sensitized solar photovoltaic cell," *Materials Today: Proceedings*, vol. 11, pp. 782–788, 2019.

[16] P. Wu, C. Liu, Y. Luo et al., "A novel black TiO_2/ZnO nanocone arrays heterojunction on carbon cloth for highly

efficient photoelectrochemical performance," *Frontiers of Materials Science*, vol. 13, no. 1, pp. 43–53, 2019.

[17] V. T. Nguyen, V. T. Vu, T. H. Nguyen, T. A. Nguyen, V. K. Tran, and P. Nguyen-Tri, "Antibacterial activity of TiO2- and ZnO-decorated with silver nanoparticles," *Journal of Composites Science*, vol. 3, no. 2, p. 61, 2019.

[18] O. V. Makarova, T. Rajh, M. C. Thurnauer, A. Martin, P. A. Kemme, and D. Cropek, "Surface modification of TiO_2 nanoparticles for photochemical reduction of nitrobenzene," *Environmental Science & Technology*, vol. 34, no. 22, pp. 4797–4803, 2000.

[19] M. G. Méndez-Medrano, E. Kowalska, A. Lehoux et al., "Surface modification of TiO_2 with Ag nanoparticles and CuO nanoclusters for application in photocatalysis," *The Journal of Physical Chemistry C*, vol. 120, no. 9, pp. 5143–5154, 2016.

[20] A. Kaiba, O. Ouerghi, M. H. Geesi et al., "Characterization and catalytic performance of Ni-Doped TiO_2 as a potential heterogeneous nanocatalyst for the preparation of substituted pyridopyrimidines," *Journal of Molecular Structure*, vol. 1203, Article ID 127376, 2020.

[21] E. S. Araújo, J. Libardi, P. M. Faia et al., "Hybrid ZnO/TiO_2 loaded in electrospun polymeric fibers as photocatalyst," *Journal of Chemistry*, vol. 2015, Article ID 476472, 10 pages, 2015.

[22] A. S. Kutuzova and T. A. Dontsova, "Characterization and properties of TiO_2-SnO_2 nanocomposites, obtained by hydrolysis method," *Applied Nanoscience*, vol. 9, no. 5, pp. 873–880, 2019.

[23] J. Prakash, S. Sun, H. C. Swart, and R. K. Gupta, "Noble metals-TiO_2 nanocomposites: from fundamental mechanisms to photocatalysis, surface enhanced Raman scattering and antibacterial applications," *Applied Materials Today*, vol. 11, pp. 82–135, 2018.

[24] A. Mishra, A. Mehta, and S. Basu, "Clay supported TiO_2 nanoparticles for photocatalytic degradation of environmental pollutants: a review," *Journal of Environmental Chemical Engineering*, vol. 6, no. 5, pp. 6088–6107, 2018.

[25] Md. H. Basha and N. O. Gopal, "Solution combustion synthesis and characterization of phosphorus doped TiO_2-CeO_2 nanocomposite for photocatalytic applications," *Materials Science and Engineering: B*, vol. 236, pp. 43–47, 2018.

[26] M. Sohail, H. Xue, Q. Jiao et al., "Synthesis of well-dispersed TiO_2/CNTs@$CoFe_2O_4$ nanocomposites and their photocatalytic properties," *Materials Research Bulletin*, vol. 101, pp. 83–89, 2018.

[27] O. Makarchuk, T. Dontsova, and A. Perekos, "Magnetic nanocomposite sorbents on mineral base," *Springer Proceedings in Physics*, vol. 195, pp. 705–719, 2017.

[28] A. A. Ismail, "Mesoporous PdO-TiO_2 nanocomposites with enhanced photocatalytic activity," *Applied Catalysis B: Environmental*, vol. 117, pp. 67–72, 2012.

[29] H. Yang, R. Shi, K. Zhang, Y. Hu, A. Tang, and X. Li, "Synthesis of WO_3/TiO_2 nanocomposites via sol-gel method," *Journal of Alloys and Compounds*, vol. 398, no. 1, pp. 200–202, 2005.

[30] A. Kutuzova, T. Dontsova, and W. Kwapinski, "TiO_2-SnO_2 nanocomposites: effect of acid-base and structural-adsorption properties on photocatalytic performance," *Journal of Inorganic and Organometallic Polymers and Materials*, vol. 80, no. 8, 2020.

[31] O. Makarchuk, T. Dontsova, A. Perekos et al., "Magnetic mineral nanocomposite sorbents for wastewater treatment," *Journal of Nanomaterials*, vol. 2017, Article ID 8579598, 7 pages, 2017.

[32] R. A. Rakkesh and S. Balakumar, "Facile synthesis of ZnO/TiO_2 core-shell nanostructures and their photocatalytic activities," *Journal of Nanoscience and Nanotechnology*, vol. 13, no. 1, pp. 370–376, 2013.

[33] P. Pascariu and M. Homocianu, "ZnO-based ceramic nanofibers: preparation, properties and applications," *Ceramics International*, vol. 45, no. 9, pp. 11158–11173, 2019.

[34] M. Kooti and A. Naghdi Sedeh, "Microwave-assisted combustion synthesis of ZnO nanoparticles," *Journal of Chemistry*, vol. 2012, Article ID 562028, 4 pages, 2012.

[35] K. Siwińska-Stefańska, A. Kubiak, A. Piasecki et al., "TiO_2-ZnO binary oxide systems: comprehensive characterization and tests of photocatalytic activity," *Materials*, vol. 11, no. 5, pp. 1–19, 2018.

[36] N. Hellen, H. Park, and K.-N. Kim, "Characterization of ZnO/TiO_2 nanocomposites prepared via the sol-gel method," *Journal of the Korean Ceramic Society*, vol. 55, no. 2, pp. 140–144, 2018.

[37] N. G. Menon, S. S. V. Tatiparti, and S. Mukherji, "Synthesis, characterization and photocatalytic activity evaluation of TiO_2-ZnO nanocomposites: elucidating effect of varying Ti: Zn molar ratio," *Colloids and Surfaces A: Physicochemical and Engineering Aspects*, vol. 565, pp. 47–58, 2019.

[38] S. Rehman, R. Ullah, A. M. Butt, and N. D. Gohar, "Strategies of making TiO_2 and ZnO visible light active," *Journal of Hazardous Materials*, vol. 170, no. 2, pp. 560–569, 2009.

[39] H. Mohammadi and M. Ghorbani, "Synthesis photocatalytic TiO_2/ZnO nanocomposite and investigation through anatase, wurtzite and $ZnTiO_3$ phases antibacterial behaviors," *Journal of Nano Research*, vol. 51, pp. 67–77, 2018.

[40] A. Kutuzova and T. Dontsova, "TiO_2-SnO_2 nanocomposites obtained by hydrothermal method," in *Proceedings of the 2018 IEEE 8th International Conference Nanomaterials: Application and Properties*, pp. 1–5, Zatoka, Ukraine, September 2018.

[41] M. A. Subhan, T. Ahmed, N. Uddin, A. K. Azad, and K. Begum, "Synthesis, characterization, PL properties, photocatalytic and antibacterial activities of nano multi-metal oxide NiO·CeO_2·ZnO," *Spectrochimica Acta Part A: Molecular and Biomolecular Spectroscopy*, vol. 136, pp. 824–831, 2015.

[42] R. Nagar and B. P. Vinayan, "Metal-semiconductor core-shell nanomaterials for energy environmental applications," *Micro And Nano Technologies*, vol. 23, pp. 99–132, 2017.

[43] A. A. Menazea and N. S. Awwad, "Antibacterial activity of TiO_2 doped ZnO composite synthesized via laser ablation route for antimicrobial application," *Journal of Materials Research and Technology*, vol. 9, 2020.

[44] J. Carbajo, A. Tolosana-Moranchel, J. A. Casas, M. Faraldos, and A. Bahamonde, "Analysis of photoefficiency in TiO_2 aqueous suspensions: effect of titania hydrodynamic particle size and catalyst loading on their optical properties," *Applied Catalysis B: Environmental*, vol. 221, pp. 1–8, 2018.

[45] S. L. In, "Comparison of photocatalytic performance of Degussa TiO_2 P25 and P90 in gas phase photocatalytic reactor," *Asian Journal of Chemistry*, vol. 23, pp. 2629–2631, 2011.

[46] J. M. Monteagudo, A. Durán, M. R. Martínez et al., "Effect of reduced graphene oxide load into TiO_2 P25 on the generation of reactive oxygen species in a solar photocatalytic reactor. Application to antipyrine degradation," *Chemical Engineering Journal*, vol. 380, Article ID 122410, 2020.

[47] A. Alonso-Tellez, R. Masson, D. Robert, N. Keller, and V. Keller, "Comparison of Hombikat UV100 and P25 TiO_2 performance in gas-phase photocatalytic oxidation reactions,"

Journal of Photochemistry and Photobiology A: Chemistry, vol. 250, pp. 58–65, 2012.

[48] J. C. Espíndola, R. O. Cristóvão, A. Mendes et al., "Photocatalytic membrane reactor performance towards oxytetracycline removal from synthetic and real matrices: suspended vs immobilized TiO_2-P25," *Chemical Engineering Journal*, vol. 378, Article ID 122114, 2019.

[49] T. A. Dontsova, E. I. Yanushevskaya, and S. V. Nahirniak, "Directional control of the structural adsorption properties of clays by magnetite modification," *Journal of Nanomaterials*, vol. 2018, Article ID 6573016, 9 pages, 2018.

[50] N. A. Abd Samad, C. W. Lai, S. B. Abd Hamid et al., "Influence applied potential on the formation of self-organized ZnO nanorod film and its photoelectrochemical response," *International Journal of Photoenergy*, vol. 2016, no. 11, 8 pages, Article ID 1413072, 2016.

[51] M. Pérez-González and S. A. Tomás, "Surface chemistry of TiO_2-ZnO thin films doped with Ag. Its role on the photocatalytic degradation of methylene blue," *Catalysis Today*, vol. 306, 2020.

[52] B. Bozkurt Çırak, B. Caglar, T. Kılınç et al., "Synthesis and characterization of ZnO nanorice decorated TiO_2 nanotubes for enhanced photocatalytic activity," *Materials Research Bulletin*, vol. 109, pp. 160–167, 2019.

[53] X. Zou, X. Dong, L. Wang et al., "Preparation of Ni doped ZnO-TiO_2 composites and their enhanced photocatalytic activity," *International Journal of Photoenergy*, vol. 2014, Article ID 893158, 8 pages, 2014.

[54] M. Thommes, K. Kaneko, A. V. Neimark et al., "Physisorption of gases, with special reference to the evaluation of surface area and pore size distribution (IUPAC Technical Report)," *Pure and Applied Chemistry*, vol. 87, no. 9, pp. 1051–1069, 2015.